UNIVERSITY OF AMSTERDAM

UvA-DARE (Digital Academic Repository)

The Mixed-Valence Catena-Heteropolycation (Bi2S2)+

Knies, M.; Nawroth, P.; Golub, P.; Isaeva, A.; Ruck, M.

Link to publication

The Mixed-Valence *Catena*-Heteropolycation (Bi$_2$S$_2$)$^+$

Maximilian Knies,[a] Paul Nawroth,[a] Pavlo Golub,[b] Anna Isaeva,[c] and Michael Ruck*[a, d]

Dedicated to Professor Josef Breu on the Occasion of his 60th Birthday.

The reaction of Bi and Bi$_2$S$_3$ in the Lewis-acidic ionic liquid [BMIm]Cl·4.3AlCl$_3$ (BMIm = 1-n-butyl-3-methylimidazolium) at 200 °C yielded air-sensitive black crystals of (Bi$_2$S$_2$)[AlCl$_4$]. X-ray diffraction on single-crystals revealed a monoclinic structure containing infinite chains $_\infty^1$(Bi$_2$S$_2$)$^+$. These polycations contain bismuth(II,III) and sulfur(-II) atoms, connected by polar covalent Bi—S and Bi—Bi bonds. The assignment of bonds is ambiguous as a distinction between primary and secondary interactions is arbitrary based on interatomic distances. A real-space quantum chemical bonding analysis, including delocalization indices, helped to quantify the interactions and charge distribution, confirming that a simple Lewis formula is inappropriate to describe the polycation.

Introduction

ILs are increasingly used in inorganic synthesis in recent years as they allow access to known materials at lower temperatures and often also higher purity compared to conventional synthesis methods.[1–13] Furthermore, ionic liquids foster the formation of new compounds that have not been accessed in other reaction media or by solvent-free reaction of the constituents. Especially complex ionic species seem to form more readily in ILs. In many cases, they are stabilized in a solid by (weakly coordinating) counter ions that are part of the IL.[5,12,13] Thus, ILs are not necessarily inert reaction media,[14,15] just as most other solvents are.

We probed ILs in the synthesis of a comparatively rare class of compounds, namely heteronuclear polycations containing pnicogen and chalcogen atoms. The first representatives were derived from N$_4$S$_4$ by *Gillespie* et al. and formed heterocycles.[16–18] For the heavier homologue phosphorus, the only known binary polycation is (P$_3$Se$_4$)$^+$, which was independently discovered by several research groups few years ago.[19] The isostructural seven-atomic cages (As$_3$S$_4$)$^{3+}$ and (As$_3$Se$_4$)$^{3+}$ had been discovered also by *Gillespie* et al.[20] The expansion towards the heavy semi-metallic elements led to the heterocubanes (Bi$_4$Ch$_4$)$^{4+}$ with Ch = S, Se, Te.[21,22] In two cases, a single bismuth vertex of the (Bi$_4$S$_4$)$^{4+}$ cube was substituted by an (AlCl)$^{2+}$ or (GaS)$^+$ dumbbell.[23,24] Also condensed polycations were isolated,[25–31] of which the largest is the quadruple *spiro*-cubane (Sb$_{13}$Se$_{16}$Br$_2$)$^{5+}$ with 31 atoms.[25]

Catena-polycations of group 16 elements have first been observed as parts of the subhalides Te$_3$Cl$_2$ and Te$_2$X (X = Cl, Br) by *Kniep* et al.[32] Subsequently, *Beck* et al. significantly expanded this compound class.[33–41] The chemical bonding in those chalcogen polycations is typically based on two-center two-electron (2c2e) bonds. Consequently, their structures combine the two- and three-fold connectivity of Ch atoms and Ch$^+$ cations, following the octet rule. Many of these chalcogen polycations are composed of rings in varying sizes, interconnected directly or bridged by one or two atoms.

Homonuclear *catena*-polycations of group 15 elements are not known. The three- and four-fold connectivity of Pn atoms and Pn$^+$ cations is expected to create highly interconnected networks. What comes closest are the infinite stripes of bismuth atoms in the subiodides Bi$_n$I$_4$ (n = 4, 14, 16, 18), in which the bismuth(II) atoms at the edges of the stripes are covalently bonded to iodine.[42] All other extended positively charged chains formed by bismuth, e.g. in Bi$_4$RuI$_2$,[43] Bi$_9$Ir$_2$I$_3$,[44] Bi$_{12}$Ni$_4$I$_3$,[45] or Bi$_{28}$Ni$_{25}$I$_5$,[46] contain transition metal atoms as an integral part of the cationic network.[47–49]

A first hint at the existence of infinite Pn-Ch polycations was reported by *Klapötke* who assumed the formation of a $_\infty^1$(PSe)$^+$ cation based on IR spectroscopic data.[50] However, a full structure elucidation is to the best of our knowledge still pending. Hence, only the two *catena*-compounds (Sb$_2$Ch$_2$)[AlCl$_4$] with Ch = Se, Te are well characterized.[51,52] They are not isostructural but their structures are rather similar. The $_\infty^1$(Sb$_2$Ch$_2$)$^+$ polycations are periodic sequences of four four-atomic rings (Sb$_2$Ch$_2$)$^+$, which are connected by Sb—Sb as well

[a] *M. Knies, P. Nawroth, Prof. Dr. M. Ruck*
Faculty of Chemistry and Food Chemistry
Technische Universität Dresden
01069 Dresden, Germany
E-mail: michael.ruck@tu-dresden.de
Homepage: https://tu-dresden.de/mn/chemie/ac/ac2
[b] *Dr. P. Golub*
Department of Theoretical Chemistry, J. Heyrovsky Institute of Physical Chemistry, 18223 Prague, Czech Republic
[c] *Prof. Dr. A. Isaeva*
Van der Waals – Zeeman Institute, Institute of Physics, University of Amsterdam, 1098 XH Amsterdam, The Netherlands
[d] *Prof. Dr. M. Ruck*
Max Planck Institute for Chemical Physics of Solids
Nöthnitzer Str. 40, 01187 Dresden, Germany

as Sb–*Ch* bonds (Figure 1). In both compounds, the counter ions are $[AlCl_4]^-$ tetrahedra, which were part of the salt melt or the ionic liquid from which the crystals precipitated.

In the case of the tellurium compound, the allocation of covalent 2c2e bonds in the polycation was solely based on interatomic Sb–Te distances. It directly led to one half of the tellurium atoms being two- and the other half three-bonded, formally bearing the positive charge of the polycation.[51] This Zintl-style interpretation is in line with the Lewis formula given for $_\infty^1(Sb_2Te_2)^+$ in Figure 1.

In $_\infty^1(Sb_2Se_2)^+$ the allocation of covalent 2c2e bonds was not possible based on Sb–Se distances alone. The cut between a bonding and a non-bonding situation would have had to be placed in the narrow gap between 307 pm and 317 pm to describe the structure with the octet rule for the electron-rich main group elements (solid lines in Figure 1a). Therefore, bonding analyses were conducted, which indeed confirmed this assignment and categorized the selenium atoms into two- and three-bonded.[52]

Herein, we report on the IL-based synthesis, the crystal structure and the chemical bonding of $(Bi_2S_2)[AlCl_4]$, which includes the first *catena*-polycation of bismuth and sulfur.

Results and Discussion

Synthesis

The reaction of Bi and Bi_2S_3 at 200 °C in the Lewis-acidic ionic liquid [BMIm]Cl·4.3AlCl_3 (BMIm = 1-*n*-butyl-3-methylimidazolium) resulted in black, air-sensitive crystals of $(Bi_2S_2)[AlCl_4]$ with sizes up to 0.5 mm. Alongside, recrystallized $AlCl_3$, $(Bi_5)[AlCl_4]_3$ and traces of a compound that could not be identified were found. To avoid the co-precipitation of $(Bi_5)[AlCl_4]_3$ is almost impossible, as bismuth polycations readily form in the IL solution. Yet, the main side products can be distinguished visually: $(Bi_5)[AlCl_4]_3$ forms red cubes and $AlCl_3$ colorless hexagonal plates. Based on a powder X-ray diffractogram (Figure S1), the estimated yield of $(Bi_2S_2)[AlCl_4]$ was 60–

70% relating to bismuth. Energy dispersive X-ray spectroscopy (EDS) confirmed the composition of the crystals.

The title compound had been previously observed as an erratically occurring, minor byproduct, only amounting to a handful of small crystals, in other syntheses containing Bi_2S_3 together with a reducing agent. The directed and comparatively efficient synthesis of $(Bi_2S_2)[AlCl_4]$ became possible by using elemental bismuth in a conproportionation reaction, yet at the prize of the co-precipitation of $Bi_5[AlCl_4]_3$.

Crystal Structure of (Bi₂S₂)[AlCl₄]

X-ray diffraction on a single-crystal of *catena*-[dibismuth(II,III) sulfur(–II)] tetrachloridoaluminate(III) at room temperature revealed a monoclinic structure in the space group $P2_1/n$ (no. 14) with eight formula units per unit cell and the lattice parameters $a = 1073.1(2)$ pm, $b = 1203.8(2)$ pm, $c = 1587.4(2)$ pm, and $\beta = 90.09(1)°$. Atomic parameters and selected interatomic distances are listed in Table 1 and Table S1 of the Supporting Information. The pseudo-orthorhombic metric promotes the formation of pseudo-merohedral twins, yet not necessarily with equal volume fractions of the twin components.

In the crystal structure of $(Bi_2S_2)[AlCl_4]$ (Figure 2), infinite chains $_\infty^1(Bi_2S_2)^+$ run along the [100] direction, separated by tetrahedral $[AlCl_4]^-$ anions. The latter can be regarded as essentially non-coordinating, except for two Bi···Cl distances of 305(2) pm and 326(2) pm, which indicate a more directed interaction between the anions and the *catena*-cation. The other Bi···Cl ($\geq 339(1)$ pm) and S···Cl distances ($\geq 343(1)$ pm) suggest mainly ionic interactions.

One of the two crystallographically independent $[AlCl_4]^-$ groups showed unusually large anisotropic displacement parameters for three of its Cl atoms, which could not be reduced sufficiently by cooling the crystal down to 250 K. Cooling below that temperature was not possible, as the
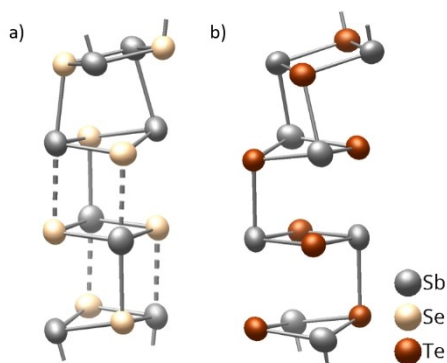

Figure 1. Characteristic segments of the *catena*-polycations in (a) $(Sb_2Se_2)[AlCl_4]$ and (b) $(Sb_2Te_2)[AlCl_4]$. Ellipsoids represent 90% probability density of atoms.

Table 1. Selected interatomic distances (*d* / pm) as well as associated bond strengths (*s*) and delocalization indices (*δ*) in $(Bi_2S_2)[AlCl_4]$. An asterisk indicates a symmetry equivalent position.

Atom pair		*d*	*s*	*δ*	Atom pair		*d*
Bi1	S1	256.9(3)	0.95	0.81	Bi3	Bi4	306.4(2)
Bi1	S1*	258.8(3)	0.90	0.80			
Bi1	S2	268.1(3)	0.70	0.64	Al1	Cl1	211.3(4)
Bi1	S3	304.8(3)	0.26	0.29	Al1	Cl2	212.2(4)
Bi2	S1	312.6(3)	0.21	0.28	Al1	Cl3	216.5(5)
Bi2	S2	254.8(3)	1.00	0.84	Al1	Cl4	213.0(5)
Bi2	S3	264.5(2)	0.77	0.64	Al2	Cl5	213.7(5)
Bi2	S4	263.7(3)	0.79	0.64	Al2	Cl6A	208(2)
Bi3	S1	335.6(3)	0.11	0.29	Al2	Cl7A	220(2)
Bi3	S2	342.1(3)	0.09	0.16	Al2	Cl8A	205(3)
Bi3	S3	260.3(2)	0.87	0.76	Al2	Cl6B	210(2)
Bi3	S4	266.5(3)	0.73	0.68	Al2	Cl7B	203(2)
Bi4	S2	292.8(3)	0.36	0.38	Al2	Cl8B	212(3)
Bi4	S3	284.1(2)	0.46	0.47			
Bi4	S4	259.9(3)	0.88	0.77			

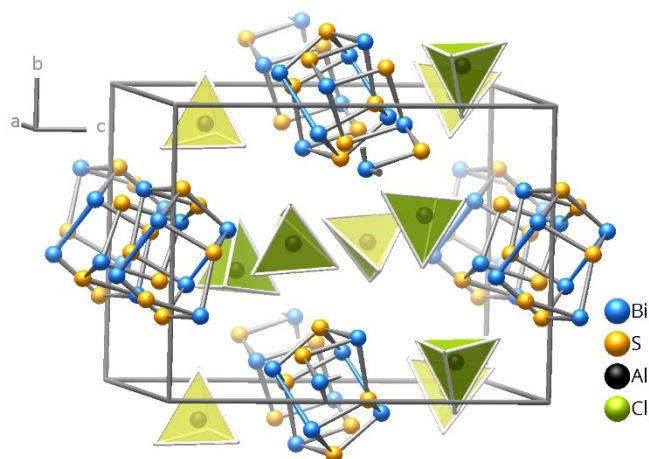**Figure 2.** Crystal structure of $(Bi_2S_2)[AlCl_4]$. For clarity only one orientation of the disordered $[AlCl_4]^-$ anion is shown.

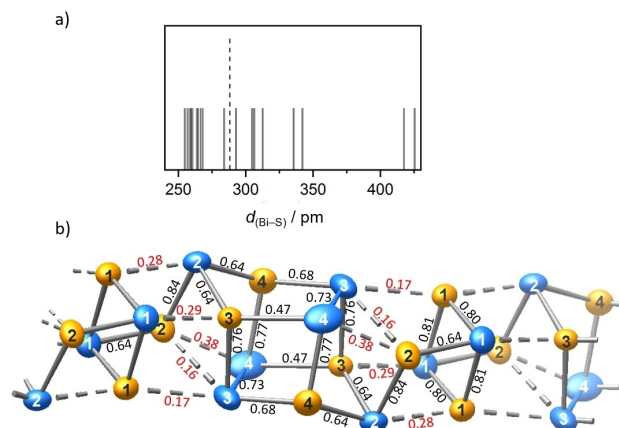**Figure 3.** a) Histogram of the Bi–S distances in the crystal structure of $(Bi_2S_2)[AlCl_4]$, the dashed line marks 285 pm. b) Section of the polycation $_\infty^1(Bi_2S_2)^+$. Distances below 285 pm are depicted as solid lines, those above are dashed. The numerical values next to the lines are the calculated DI values. The colour code demarcates the primary (black, δ higher or equal to 0.5) and secondary (red, δ < 0.5) bonds. Ellipsoids enclose 90% of the probability density of the atoms.

intensity of the Bragg reflections was reduced drastically at lower temperatures. To model the rotational disorder at room temperature, atomic split positions were introduced, which refined close to and were then set to a probability of 50% each. The Al–Cl distances range from 211.3(4) pm to 216.5(5) pm for the ordered tetrahedron, which is in accordance with the distances observed in Na[AlCl_4].[53] For the disordered $[AlCl_4]^-$ anion the range of distances is significantly wider [203(2)–220(2) pm]. However, due to the close proximity of the atomic split positions, these distances are less reliable than those for the regular tetrahedron.

The more interesting part of the compound is the *catena*-polycation $_\infty^1(Bi_2S_2)^+$, which structure needs four formula units to be described. Its composition and charge indicate a mixed valence species. In fact, Bi1 and Bi2 bind only to sulfur atoms and can thus be identified as bismuth(III), while Bi3 and Bi4 bind to each other in a dumbbell and are thus bismuth(II). The Bi3–Bi4 distance of 306.4(1) pm falls in the range observed for Bi_2^{4+} dumbbells in heteropolar solids[54–57] [e.g. 306.3(3) pm in $Cu_3Bi_2S_3Br_2$[40]], but is about 2% longer than Bi–Bi single bonds in organometallic compounds.[58,59]

In the histogram of Bi–S distances (Figure 3), those significant for chemical bonding group between 254.8(3) pm and 344.8(3) pm, are clearly separated from the insignificant (>415 pm). For comparison, the Bi–S bond length in the bipyramidal Bi_2S_3 molecule in $M_2Bi_2S_3[AlCl_4]_2$ (M = Ag, Cu)[60] range from 260.9(2) pm to 265.2(1) pm, which is in accordance with the majority of the Bi–S distances found in the title compound. Similar distances were observed for three-bonded bismuth atoms in discrete sulfidobismuth polycations, such as $(Bi_4S_4)^{4+}$ [263.7(3)–269.7(3) pm][21] or $(Bi_7S_8)^{5+}$ [259.1(3)–

267.2(2) pm].[28] For the network in the standard modification of Bi_2S_3, a distinction can be made between primary [259.0–273.8 pm] and secondary [297.5–338.6 pm] Bi–S bonds,[61,62] matching the distance range observed for $(Bi_2S_2)[AlCl_4]$ quite well.

When all distances up to 344.8(3) pm are represented as bonds, the polycation $_\infty^1(Bi_2S_2)^+$ appears as a periodic sequence of edge- and face-sharing cubes (Figure 3). Since most of the bond angles are close to 90°, which is typical for 2c2e bonds of heavy p-elements, or 180°, which points at a 3c4e bond (using both lobes of a *p* orbital at the central atom), stronger and weaker covalent bonds seem to coexist. Hence, it is not straight forward which interatomic distance corresponds to an interaction that justifies to draw a bond in the graphical representation and where we should place the positive formal charge. In Figure 3, the solid lines represent distances up to 284 pm, which fulfills the octet rule based on 2c2e bonds. All bismuth atoms have three bonds, S1 and S2 have two bonds, while S3 and S4 have three bonds and as pseudo-elements of group 15 bear the formal charge. Yet, with regard to the histogram of interatomic Bi–S distances, this seems to be a rather arbitrary cut and assignment.

Using the empirical bond-length bond-strength correlation by *Brese* and *O'Keeffe* with the tabulated bond valence parameter R_{BiS} = 255 pm, bond valence sums $v = \Sigma s_{BiS}$ of 1.70 and 1.80 for bismuth(II) but 2.77 and 2.81 for bismuth(III) result and confirm the assigned oxidation states (Table 1 and 2). The bond valence sums for S1 (2.17) and S2 (2.15) are about 10% smaller than for S3 (2.36) and S4 (2.40). Although this differentiation is small, it supports the tentative assignment of the trivalent state to S3 and S4 as derived from the 2c2e picture.

Table 2. Oxidation state OS, assigned formal charge FC, expected number N of Bi–S bonds (octet rule), calculated QTAIM charges Q, bond valence sum $v = \Sigma s_{BiS}$, and sum of delocalization indices $\Sigma\delta_{BiS}$ for the atoms in the $(Bi_2S_2)^+$ polycation.

Atom	OS	FC	N_{BiS}	Q	v_{BiS}	$\Sigma\delta_{BiS}$
Bi1	III	0	3	+1.35	2.81	2.54
Bi2	III	0	3	+1.40	2.77	2.40
Bi3	II	0	2	+1.00	1.80	1.61
Bi4	II	0	2	+1.07	1.70	1.63
S1	−II	0	2	−0.75	2.17	2.06
S2	−II	0	2	−0.80	2.15	2.02
S3	−II	+	3	−0.80	2.36	2.16
S4	−II	+	3	−0.70	2.40	2.35

Based on density functional theory (DFT), we performed a real space bonding analysis of the entire structure. Partial charges for the atoms were calculated according to the Quantum Theory of Atoms in Molecules (QTAIM).[63] For the evaluation of bonding the delocalization index (DI, δ) between the QTAIM atoms was employed.[64–66] It represents the positional space analogue to the bond order definition of the Wiberg and the Mayer bond index[67,68] and can be regarded as a quantification of the bond order ($\delta = 1$ for non-polar covalent bonding).

The DI values for the $[AlCl_4]^-$ tetrahedra fall into the range $\delta(Al,Cl) = 0.25–0.29$, while the computed formal charges $Q(Al) = +2.4$ and $Q(Cl) = -0.8$. This bonding situation can be described as a polar covalent bond, since for ionic bonds, e.g. in $NaCl$[80] the DIs are much lower $\delta(Na,Cl) = 0.07$ for the similarly large QTAIM charges. The interactions between the polycation and the anions are characterized by $\delta(Bi,Cl) = 0.12$. Preliminary band structure calculations reveal a gapped electronic spectrum in $(Bi_2S_2)[AlCl_4]$ (bulk band gap estimated as 0.6 and 1.4 eV by DFT GGA and LDA, respectively). In this scenario it is justifiable to compare the weak electrostatic Bi–Cl interactions to the electrostatic bonding in $NaCl$.[80] The obtained values are very close to those computed for the corresponding interactions in $(Sb_2Se_2)[AlCl_4]$, viz. $\delta(Al,Cl) = 0.26–0.27$ and $\delta(Sb,Cl) = 0.17$,[52] indicating a very similar bonding pattern.

For the $(Bi_2S_2)^+$ polycation, the calculated partial charges of the sulfur atoms (Table 2) range between −0.7 and −0.8, indicating no substantial differentiation between them. In line with their electronegativity, all of them are negatively charged, which again points out how thoughtful formal charges must be interpreted. The QTAIM charges for the cations are +1.4 for the bismuth(III) atoms, but only +1.0 or +1.1 for the bismuth(II) atoms. Following the differences in electronegativity, the polarity is more pronounced in $(Bi_2S_2)^+$ than in $(Sb_2Se_2)^+$, in which the selenium atoms have a charge of about −0.5.[52]

The DIs between the neighboring atoms are included in Figure 3. The DI of the covalent Bi–Bi bond is $\delta(Bi,Bi) = 0.73$. This correlates with the distance that is somewhat longer than expected for a single bond and could be a consequence of the positive partial charges (reduced electron density) of the bismuth atoms. The DIs for the Bi–S interactions spread between 0.84 and 0.16 following the trend of interatomic

distances, however, with some differences to the empirical bond strengths s_{BiS}. For the 2c2e bonding model, which can be represented in a Lewis formula, the cut-off is between $\delta(Bi,S) = 0.47$ and 0.38, i.e. in a similar way arbitrary as for the associated bond lengths. The almost linear three-atomic segments around bismuth atoms (S1–Bi1–S3; S4–Bi2–S1; S4–Bi3–S1; S3–Bi4–S2) are reminiscent of 3c2e bonding, but unlike in 3c2e bonds, the DI values between the terminal atoms are very low (cf. 0.14 for Te_3[69] and 0.02 for S4–Bi3–S1).

Regardless of their interpretation, the DI values for the Bi–S interactions are notably smaller in the absolute values than those calculated for 2c2e or 3c4e bonds in homonuclear arrangements such as I_3^-, Cl_3^- or the Te_{10} molecule.[69] We attribute the difference to the electrostatic part of the polar bond between bismuth and sulfur. Despite the influence of bond polarity, the sum of delocalization indices $\delta(Bi,S)$ in which a particular atom of the polycation is involved should be correlated to its valence. In fact, $\Sigma\delta(Bi,S)$ (Table 2) shows the same characteristics as discussed above for the bond valence sum $v = \Sigma s_{Bi-S}$. In particular, chemically similar atoms have similar $\Sigma\delta(Bi,S)$, regardless of the summands.

A final remark: In the presented structure model, the displacement ellipsoid of Bi4 is larger than those of the other bismuth atoms. It is possible to refine Bi4 with split positions, Bi4a (62%) and Bi4b (38%, Table S2 and S3), which increases the gap between "bonding" and "non-bonding" distances from 9 to 30 pm (Bi4a–S3 274(2) pm, Bi4a···S2 304(2) pm; Bi4b···S3 302(2) pm, Bi4b–S2 274(2) pm). This differentiated description assigns the positive formal charge alternatingly to S3 or S2.

Conclusions

$(Bi_2S_2)[AlCl_4]$, which was synthesized in an IL, includes the first periodic sulfidobismuth polycation. In $_\infty^1(Bi_2S_2)^+$, bismuth and sulfur atoms are connected through covalent Bi–S and Bi–Bi bonds. The description of bonding in the heteropolycation by a Lewis formula with only 2c2e bonds is not appropriate. Substantial secondary interactions between bismuth and sulfur atoms are indicated simply by the observed interatomic distances and, much more sophisticated, by calculated delocalization indices. Moreover, the effective charge distribution differs fundamentally from the assignment of positive formal charges to three-bonded sulfur atoms in the Lewis formula.

Experimental Section

Synthesis: All compounds were handled in an argon-filled glove box (MBraun; $p(O_2)/p^0 < 1$ ppm, $p(H_2O)/p^0 < 1$ ppm). The reactions were carried out in silica ampules with a length of 120 mm and a diameter of 14 mm. $(Bi_2S_2)[AlCl_4]$ was synthesized in the Lewis-acidic ionic liquid [BMIm]Cl·4.3AlCl₃, which acted as solvent and reactant. In a typical experiment, the ampule was loaded with 52.3 mg Bi (99.9%, abcr, treated twice with H_2 at 220°C), 128.6 mg Bi_2S_3 (99.9%, Alfa Aesar), 90.0 mg [BMIm]Cl (98%, Sigma Aldrich, dried under vacuum at 100°C), and 300.0 mg AlCl₃ (sublimed three times). The evacuated and sealed ampule was heated at 200°C for 6 days. The solution turned black at this temperature. Before

ZAAC
Journal of Inorganic and General Chemistry
Zeitschrift für anorganische und allgemeine Chemie

ARTICLE

cooling the mixture to room temperature at $\Delta T/t = -6\,\mathrm{K\,h^{-1}}$, the ampule was tilted to enable the separation of already precipitated byproducts. Black crystals of **1** were obtained in sizes from approximately 50 to 500 μm, in an estimated yield of 60–70%, alongside red $Bi_5[AlCl_4]_3$ and colorless $AlCl_3$. The crystals of **1** were identified visually, according to their color and shape, and separated mechanically from other crystalline species and most of the IL. No further treatment was applied to these crystals, as the small amounts of residual IL on the crystal surface did not impede the following investigations.

Chemical analysis: EDX spectroscopy was conducted using a SU8020 (Hitachi) SEM equipped with a Silicon Drift Detector (SDD) X–Max^N (Oxford) to check the chemical composition of the crystals. However, interpretation of the measured data was impeded by the partial decomposition of the $[AlCl_4]^-$ ions in the high-energetic electron beam ($U_a = 20$ kV) that is necessary to activate bismuth for this measurement.[70] Furthermore, the air-sensitivity prevented polishing of the surface, resulting in lower accuracy of the measured data. Still, we were able to confirm the qualitative composition as well as the ratio of bismuth to sulfur within the margin of error under these conditions. Calcd./exp. Bi:S:Al:Cl (at.-%) in $(Bi_2S_2)[AlCl_4]$: 22.2:22.2:11.1:44.4/26(4):22(4):6(1):36(5).

Powder X-ray diffraction: Data collection was performed at 296(3) K with an X'Pert Pro MPD diffractometer (PANalytical) equipped with a Ge(220) hybrid-monochromator using Cu-$K_{\alpha 1}$ radiation ($\lambda = 154.056$ pm). Due to their sensitivity to moisture, the samples were contained in a glass capillary (Hilgenberg) with an outer diameter of 0.3 mm.

X-ray crystal structure determination: Single-crystal X-ray diffraction was measured on a four-circle Kappa APEX II CCD diffractometer (Bruker) with a graphite(002)-monochromator and a CCD-detector at $T = 296(2)$ K. Mo-K_α radiation ($\lambda = 71.073$ pm) was used. A numerical absorption correction based on an optimized crystal description was applied,[71] and the initial structure solution was performed in JANA2006.[72] The structure was refined in SHELXL against F_o^2.[73–75]

$(Bi_2S_2)[AlCl_4]$: monoclinic; space group $P2_1/n$ (no. 14); $T = 296(2)$ K; $a = 1073.1(2)$ pm, $b = 1203.8(2)$ pm, $c = 1587.4(2)$ pm, $\beta = 90.09(1)°$; $V = 2050.7(3) \times 10^6$ pm^3; $Z = 8$; $\rho_{calcd.} = 4.216$ g cm^{-3}; μ(Mo-K_α) $= 35.7$ mm^{-1}; $2\theta_{max} = 55.3°$, $-14 \leq h \leq 14$, $-15 \leq k \leq 15$, $-20 \leq l \leq 20$; 28161 measured, 4769 unique reflections, $R_{int} = 0.098$, $R_\sigma = 0.065$; 192 parameters, $R_1(3712\ F_o > 4\sigma(F_o)) = 0.038$, wR_2(all F_o^2) $= 0.069$, $GooF = 1.041$, min./max. residual electron density: $-2.23/1.84$ e$\times$10^{-6} pm^{-3}. For atomic parameters see Table S2 of the Supporting Information.

Further details of the crystal structure determination are available from the Fachinformationszentrum Karlsruhe, D-76344 Eggenstein-Leopoldshafen (Germany), E-mail: crysdata@fiz-karlsruhe.de, on quoting the depository number CSD-2086520.

Quantum chemical calculations: Scalar-relativistic first-principles calculations for the periodic structure of $(Bi_2S_2)[AlCl_4]$ were performed in the program package ABINIT[76] version 7.8.2 utilizing the PAW method[77] and generalized gradient approximation (GGA) with the revised Perdew-Burke-Ernzerhof (PBEsol)[78] functional. A $3\times3\times2$ k-point grid was used for the DI calculations and for self-consistent energy calculations with LDA, a $4\times4\times3$ k-point grid was used for self-consistent energy band calculations with GGA. The plane-wave energy cutoff was set to 18 Hartree. 5 valence electrons were considered for Bi atom, 6 for S atom, 3 for Al, and 7 for Cl. We used experimental unit cell parameters and atomic coordinates without relaxation. Formal atomic charges were computed by topological analysis of the converged electron density (partitioning of the gradient field into basins and their integration) according to

the quantum theory of atoms in molecules (QTAIM) by Bader[63] within the DGrid code.[79] Delocalization indices[64–66] were evaluated by partitioning of the electron pair density in real space over the computed QTAIM basins within the DGrid code. For these calculations, a modified version of DGrid-4.6 software was used; we utilized an ABINIT module that was described in [80] and used in [81].

Conflict of Interest

The authors declare no conflict of interest.

[1] D. Freudenmann, S. Wolf, M. Wolff, C. Feldmann, *Angew. Chem.* **2011**, *123*, 11244–11255; *Angew. Chem. Int. Ed.* **2011**, *50*, 11050–11060.
[2] E. Ahmed, J. Breternitz, M. F. Groh, M. Ruck, *CrystEngComm* **2012**, *14*, 4874–4885.
[3] M. F. Groh, U. Müller, E. Ahmed, A. Rothenberger, M. Ruck, *Z. Naturforsch. B* **2014**, *68*, 1108–1122.
[4] J. Estager, J. D. Holbrey, M. Swadźba-Kwaśny, *Chem. Soc. Rev.* **2014**, *43*, 847–886.
[5] M. F. Groh, A. Wolff, M. A. Grasser, M. Ruck, *Int. J. Mol. Sci.* **2016**, *17*, 1452.
[6] P. Wasserscheid, T. Welton, *Ionic Liquids in Synthesis*, Wiley, **2008**.
[7] M. Antonietti, D. Kuang, B. Smarsly, Y. Zhou, *Angew. Chem.* **2004**, *116*, 5096–5100; *Angew. Chem. Int. Ed.* **2004**, *43*, 4988–4992.
[8] Z. Ma, J. Yu, S. Dai, *Adv. Mater.* **2010**, *22*, 261–285.
[9] X. Duan, J. Ma, J. Lian, W. Zheng, *CrystEngComm* **2014**, *16*, 2550–2559.
[10] X. Kang, X. Sun, B. Han, *Adv. Mater.* **2016**, *28*, 1011–1030.
[11] A. Wolff, T. Doert, J. Hunger, M. Kaiser, J. Pallmann, R. Reinhold, S. Yogendra, L. Giebeler, J. Sichelschmidt, W. Schnelle, R. Whiteside, H. Q. N. Gunaratne, P. Nockemann, J. J. Weigand, E. Brunner, M. Ruck, *Chem. Mater.* **2018**, *30*, 7111–7123.
[12] E. Ahmed, M. Ruck, *Coord. Chem. Rev.* **2011**, *255*, 2892–2903.
[13] S. Santner, J. Heine, S. Dehnen, *Angew. Chem.* **2016**, *128*, 886–904; *Angew. Chem. Int. Ed.* **2016**, *55*, 876–893.
[14] T. Zhang, K. Schwedtmann, J. J. Weigand, T. Doert, M. Ruck, *Chem. Eur. J.* **2018**, *24*, 9325–9332.
[15] S. Sowmiah, V. Srinivasadesikan, M.-C. Tseng, Y.-H. Chu, *Molecules* **2009**, *14*, 3780–3813.
[16] R. J. Gillespie, P. R. Ireland, J. E. Vekris, *Can. J. Chem.* **1975**, *53*, 3147–3152.
[17] R. J. Gillespie, D. R. Slim, J. D. Tyrer, *J. Chem. Soc. Chem. Commun.* **1977**, 253–255.

[18] R. J. Gillespie, J. P. Kent, J. F. Sawyer, *Inorg. Chem.* **1981**, *20*, 3784–3799.

[19] K.-O. Feldmann, T. Wiegand, J. Ren, H. Eckert, J. Breternitz, M. F. Groh, U. Müller, M. Ruck, B. Maryasin, C. Ochsenfeld, O. Schön, K. Karaghiosoff, J. J. Weigand, *Chem. Eur. J.* **2015**, *21*, 9697–9712.

[20] B. H. Christian, R. J. Gillespie, J. F. Sawyer, *Inorg. Chem.* **1981**, *20*, 3410–3420.

[21] J. Beck, S. Schlüter, N. Zotov, *Z. Anorg. Allg. Chem.* **2004**, *630*, 2512–2519.

[22] J. Beck, M. Dolg, S. Schlüter, *Angew. Chem.* **2001**, *113*, 2347–2350; *Angew. Chem. Int. Ed.* **2001**, *40*, 2287–2290.

[23] M. F. Groh, A. Isaeva, U. Müller, P. Gebauer, M. Knies, M. Ruck, *Eur. J. Inorg. Chem.* **2016**, *6*, 880–889.

[24] D. Freudenmann, C. Feldmann, *Dalton Trans.* **2010**, *40*, 452–456.

[25] E. Ahmed, J. Breternitz, M. F. Groh, A. Isaeva, M. Ruck, *Eur. J. Inorg. Chem.* **2014**, *2014*, 3037–3042.

[26] E. Ahmed, A. Isaeva, A. Fiedler, M. Haft, M. Ruck, *Chem. Eur. J.* **2011**, *17*, 6847–6852.

[27] Q. Zhang, I. Chung, J. I. Jang, J. B. Ketterson, M. G. Kanatzidis, *J. Am. Chem. Soc.* **2009**, *131*, 9896–9897.

[28] M. Knies, M. F. Groh, T. Pietsch, M. Lê Anh, M. Ruck, *ChemistryOpen* **2021**, *10*, 110–116.

[29] A. Eich, W. Hoffbauer, G. Schnakenburg, T. Bredow, J. Daniels, J. Beck, *Eur. J. Inorg. Chem.* **2014**, *2014*, 3043–3052.

[30] A. Eich, S. Schlüter, G. Schnakenburg, J. Beck, *Z. Anorg. Allg. Chem.* **2013**, *639*, 375–383.

[31] K. Biswas, Q. Zhang, I. Chung, J.-H. Song, J. Androulakis, A. J. Freeman, M. G. Kanatzidis, *J. Am. Chem. Soc.* **2010**, *132*, 14760–14762.

[32] R. Kniep, D. Mootz, A. Rabenau, *Z. Anorg. Allg. Chem.* **1976**, *422*, 17–38.

[33] J. Beck, *Angew. Chem.* **1991**, *103*, 1149–1151; *Angew. Chem. Int. Ed. Engl.* **1991**, *30*, 1128–1130.

[34] J. Beck, *Z. Anorg. Allg. Chem.* **1993**, *619*, 237–242.

[35] J. Beck, G. Bock, *Z. Anorg. Allg. Chem.* **1994**, *620*, 1971–1975.

[36] J. Beck, J. Richter, M. A. Pell, J. A. Ibers, *Z. Anorg. Allg. Chem.* **1996**, *622*, 473–478.

[37] G. W. Drake, G. L. Schimek, J. W. Kolis, *Inorg. Chem.* **1996**, *35*, 1740–1742.

[38] J. Beck, T. Schlörb, *Phosphorus Sulfur Silicon Relat. Elem.* **1997**, *124*, 305–313.

[39] J. Beck, A. Stankowski, *Z. Naturforsch. B* **2001**, *56*, 453–457.

[40] J. Beck, A. Fischer, A. Stankowski, *Z. Anorg. Allg. Chem.* **2002**, *628*, 2542–2548.

[41] C. Feldmann, D. Freudenmann, *Acta Crystallogr. Sect. C* **2012**, *68*, i68–i70.

[42] A. Weiz, M. Lê Anh, M. Kaiser, B. Rasche, T. Herrmannsdörfer, T. Doert, M. Ruck, *Eur. J. Inorg. Chem.* **2017**, *2017*, 5609–5615.

[43] M. Ruck, *Z. Anorg. Allg. Chem.* **1997**, *623*, 1583–1590.

[44] M. Ruck, R. M. Heich, *Z. Anorg. Allg. Chem.* **2000**, *626*, 2449–2456.

[45] M. Ruck, *Z. Anorg. Allg. Chem.* **1997**, *623*, 243–249.

[46] M. Ruck, *Z. Anorg. Allg. Chem.* **1995**, *621*, 2034–2042.

[47] M. Ruck, *Ref. Module Chem. Mol. Sci. Chem. Eng.*, Elsevier, **2015**.

[48] M. Ruck, *Z. Kristallogr.* **2010**, *225*, 167–172.

[49] M. Ruck, *Angew. Chem.* **2001**, *113*, 1222–1234; *Angew. Chem. Int. Ed.* **2001**, *40*, 1182–1193.

[50] T. M. Klapötke, C. M. Rienäcker, *Z. Anorg. Allg. Chem.* **1994**, *620*, 2104–2107.

[51] J. Beck, S. Schlüter, *Z. Anorg. Allg. Chem.* **2005**, *631*, 569–574.

[52] M. F. Groh, J. Breternitz, E. Ahmed, A. Isaeva, A. Efimova, P. Schmidt, M. Ruck, *Z. Anorg. Allg. Chem.* **2015**, *641*, 388–393.

[53] N. C. Baenziger, *Acta Crystallogr.* **1951**, *4*, 216–219.

[54] A. Heerwig, M. Ruck, *Z. Anorg. Allg. Chem.* **2011**, *637*, 1814–1817.

[55] R. Groom, A. Jacobs, M. Cepeda, R. Drummey, S. E. Latturner, *Chem. Mater.* **2017**, *29*, 3314–3323.

[56] B. Wahl, M. Ruck, *Z. Anorg. Allg. Chem.* **2008**, *634*, 2873–2879.

[57] W. Yin, D. Mei, J. Yao, P. Fu, Y. Wu, *J. Solid State Chem.* **2010**, *183*, 2544–2551.

[58] H. J. Breunig, *Z. Anorg. Allg. Chem.* **2005**, *631*, 621–631.

[59] L. Balázs, H. J. Breunig, *Coord. Chem. Rev.* **2004**, *248*, 603–621.

[60] M. F. Groh, M. Knies, A. Isaeva, M. Ruck, *Z. Anorg. Allg. Chem.* **2015**, *641*, 279–284.

[61] V. Kupčík, L. Veselá-Nováková, *Tschermaks Mineral. Petrogr. Mitt.* **1970**, *14*, 55–59.

[62] L. F. Lundegaard, E. Makovicky, T. Boffa-Ballaran, T. Balic-Zunic, *Phys. Chem. Miner.* **2005**, *32*, 578–584.

[63] R. F. W. Bader, *Atoms in Molecules: A Quantum Theory*, Oxford University Press, Oxford, **1994**.

[64] J. G. Angyan, M. Loos, I. Mayer, *J. Phys. Chem.* **1994**, *98*, 5244–5248.

[65] R. F. W. Bader, A. Streitwieser, A. Neuhaus, K. E. Laidig, P. Speers, *J. Am. Chem. Soc.* **1996**, *118*, 4959–4965.

[66] X. Fradera, M. A. Austen, R. F. W. Bader, *J. Phys. Chem. A* **1999**, *103*, 304–314.

[67] K. B. Wiberg, *Tetrahedron* **1968**, *24*, 1083–1096.

[68] I. Mayer, *Chem. Phys. Lett.* **1983**, *97*, 270–274.

[69] A. Günther, A. Isaeva, M. Ruck, *Z. Anorg. Allg. Chem.* **2012**, *638*, 2521–2525.

[70] U. Müller, A. Isaeva, J. Richter, M. Knies, M. Ruck, *Eur. J. Inorg. Chem.* **2016**, *2016*, 3580–3584.

[71] *X-Shape, Crystal Optimization for Numerical Absorption Correction Program*, Stoe & Cie GmbH, Darmstadt, Germany, **2008**.

[72] V. Petricek, M. Dusek, L. Palatinus, *JANA2006, The Crystallographic Computing System*, Institute Of Physics, Praha, Czech Republic, **2011**.

[73] G. M. Sheldrick, *Acta Crystallogr. Sect. A* **2008**, *64*, 112–122.

[74] G. M. Sheldrick, *SHELXL, Program for Crystal Structure Refinement − Multi-CPU*, Georg-August-Universität Göttingen, Göttingen, Germany, **2014**.

[75] G. M. Sheldrick, *Acta Crystallogr. Sect. A* **2015**, *71*, 3–8.

[76] X. Gonze, B. Amadon, P.-M. Anglade, J.-M. Beuken, F. Bottin, P. Boulanger, F. Bruneval, D. Caliste, R. Caracas, M. Côté, T. Deutsch, L. Genovese, P. Ghosez, M. Giantomassi, S. Goedecker, D. R. Hamann, P. Hermet, F. Jollet, G. Jomard, S. Leroux, M. Mancini, S. Mazevet, M. J. T. Oliveira, G. Onida, Y. Pouillon, T. Rangel, G.-M. Rignanese, D. Sangalli, R. Shaltaf, M. Torrent, M. J. Verstraete, G. Zerah, J. W. Zwanziger, *Comput. Phys. Commun.* **2009**, *180* (12), 2582–2615.

[77] P. E. Blöchl, *Phys. Rev. B* **1994**, *50* (24), 17953–17979.

[78] J. P. Perdew, A. Ruzsinszky, G. I. Csonka, O. A. Vydrov, G. E. Scuseria, L. A. Constantin, X. Zhou, K. Burke, *Phys. Rev. Lett.* **2008**, *100* (13), 136406.

[79] M. Kohout, DGrid-4.6, **2012**, Radebeul.

[80] P. Golub. Chemical bonding analysis of complex solids in real space from the projector augmented-wave method. Dissertation, Technische Universität Dresden, 2017. In particular, we adopted the algorithm implemented by P. Golub and A. Baranov for the PAW method as a general-purpose module of the program DGrid interfaced to the output of ABINIT code. The developed code for the ABINIT module and the modified version of DGrid-4.6 are available upon request.

[81] P. Golub, A. I. Baranov, *J. Chem. Phys.* **2016**, *145*, 154107.